# Electric Propulsion at Space Systems/Loral

## IEPC-2009-270

Ronald L. Corey[1] and David J. Pidgeon[2]
*Space Systems/Loral, Palo Alto, CA, 94303*

**Space Systems/Loral has extensive experience with electric propulsion dating back to the early 1990's when an agreement was made to develop the newly available Russian manufactured SPT-100 for use on western communications satellites. Space Systems/Loral to date has launched five spacecraft with SPT-100 electric propulsion subsystems, with nine more satellites with this subsystem currently under construction. The SPT subsystem provides impulse for on-orbit inclination, eccentricity control, and momentum wheel unloads. The western qualification and integration of the SPT-100 subsystem onto Space Systems/Loral spacecraft was completed in 2001 with the first flight in 2004. Since the initial three satellites launched in 2004/2005, an additional two spacecraft have been launched in 2009. The SPT subsystem now has more than thirteen years of cumulative on orbit experience, with a single thruster accumulating over 5 years of near-daily operation in orbit. This paper summarizes Space Systems/Loral's experience from the western qualification of the SPT-100 subsystem to successful on-orbit operation. Included are a description of hardware qualification, modeling and analysis with on-orbit results compared to predictions for thruster performance, and spacecraft interactions such as electromagnetic interference, plume effects on solar arrays, and thermal control surfaces.**

## I.    Introduction

SPACE SYSTEMS/LORAL (SS/L) has implemented the Stationary Plasma Thruster (SPT-100) onto spacecraft for primary north-south station keeping (NSSK). The SPT-100 is a Hall-effect thruster designed and built in Russia by the Experimental Design Bureau Fakel which has over 15 years of on orbit flight heritage on Russian spacecraft with this thruster. In 1991, SS/L and Fakel formed the joint venture International Space Technology, Inc. (ISTI) with the objective to qualify the SPT-100 to accepted western standards, and to qualify a power processor unit (PPU) using accepted Mil-Standard space qualified components. Use of the SPT-100 allows substantial reductions in on-board propellant mass and commensurate increased life compared with an equivalent chemical propulsion system. The SPT-100 subsystem, as implemented on SS/L spacecraft, provides impulse for on-orbit inclination and eccentricity control as well as momentum wheel unloads.

The SPT subsystem, as shown in Figs. 1 and 2, contains four SPT-100s, eight xenon flow controllers (XFC-100s), two PPUs, two xenon storage tanks, and a propellant management assembly (PMA) [1]. There are several references describing the design and operation of Hall thrusters in the literature so no detailed description will be given here. There are excellent textbooks on Hall thrusters in general [2] and for SPTs in particular [3]. The SPT-100, as implemented on SS/L spacecraft, has a discharge power of 1.35 kW, a discharge voltage of 300 V and is equipped with a fully redundant cathode. The XFCs manufactured by Fakel consist of three solenoid valves, a thermothrottle for fine regulation of the propellant flow and orifices to split the flow between the anode and cathode at the ratio 13:1. The PPU manufactured by SS/L controls the thermothrottle to regulate the discharge current which is typically set at $4.5 \pm 0.1$ A. The PPU provides power to energize, monitor, and control the SPT and its associated XFC.

---

[1] SPT Subsystem Responsible Engineer, 3825 Fabian Way MS G-86.
[2] Executive Director, 3825 Fabian Way MS G-44.

Power input is from the spacecraft 100 V regulated bus.  As shown in Fig. 2 the PPU can operate two SPTs, one SPT at a time, by utilizing high-voltage relays.  For any single operation, the PPU output is directed to either the primary or the redundant cathode side of either of two SPTs.  The PPU is commanded by the spacecraft computer, which also processes all PPU telemetry.  The xenon storage tanks manufactured by General Dynamics are carbon over wrapped pressure vessels (COPV) with a maximum expected operating pressure (MEOP) of 2700 psia.  The PMA manufactured by Moog contains parallel redundant normally closed (NC) pyrotechnic valves to isolate the xenon tanks during ground operations and launch. Downstream of the pyrotechnic valves are parallel redundant strings of solenoid type latch valves and single stage bellows-type regulators.  The regulators operate at 37 ± 1.45 psia.  The PMA also includes three pressure transducers to allow for system health monitoring and propellant usage.

Typically a pair of SPTs (primary and redundant) are located on both the north and south faces of the satellite, and are canted between 30° and 40° from the deployed solar array as shown in Fig 3.  Daily NSSK maneuvers are performed in two segments; a north and a south firing, separated by approximately 12 hours. During a maneuver, the direction of thrust, by way of momentum wheels speeds, is closely monitored by the spacecraft attitude control subsystem and a two-axis mechanism makes real-time adjustments.

SS/L has successfully launched five SPT-equipped spacecraft to date with nine more under construction.  Figure 4 shows all the SS/L manufactured SPT equipped spacecraft in order of launch date or projected launch date.  It is interesting to note the diversity of spacecraft bus configurations for which SPTs have been used as shown in Fig. 4.  Spacecraft shown with more solar array panels are obviously higher power spacecraft and tend to be bigger and heavier which leads to longer SPT burn times.  Smaller spacecraft have also been constructed with SPTs where the SPTs were mission enabling for a lower capability launch vehicles.  The first SPT-equipped spacecraft launched in 2009, is an example of smaller satellites for which the SPT-100 subsystem was mission enabling as it launched on a Land Launch Xenit-3SLB.
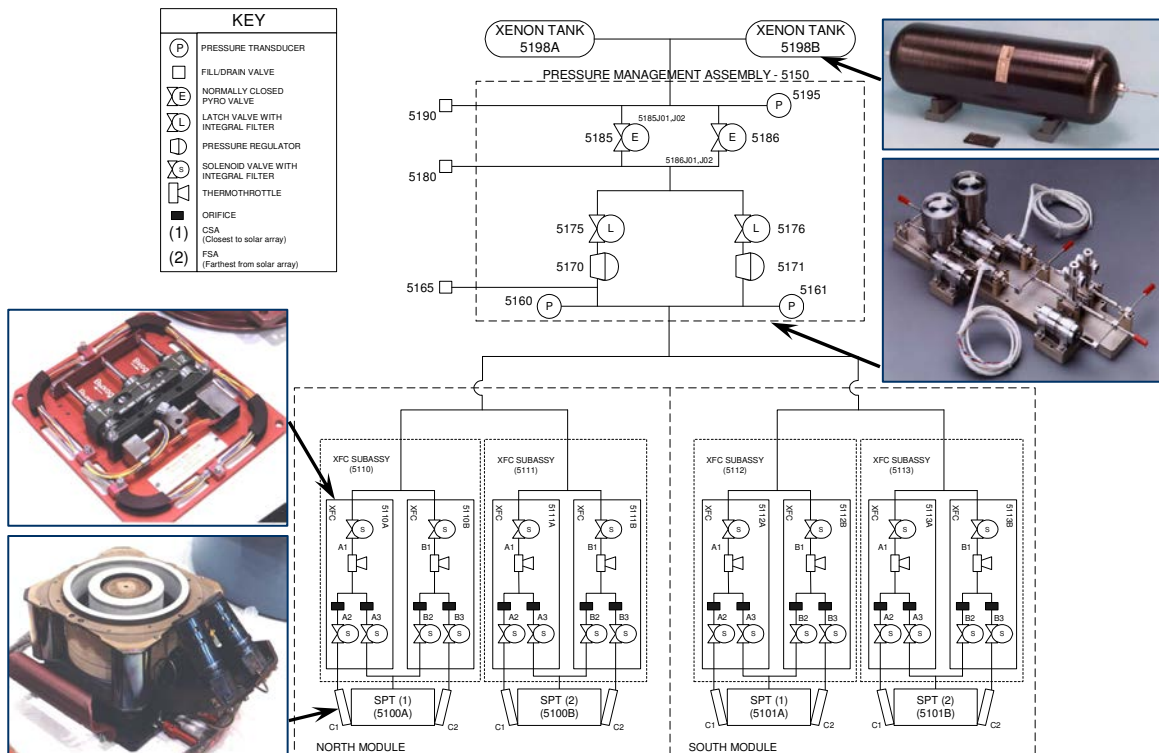


**Figure 1.  SPT subsystem pneumatic block diagram.**
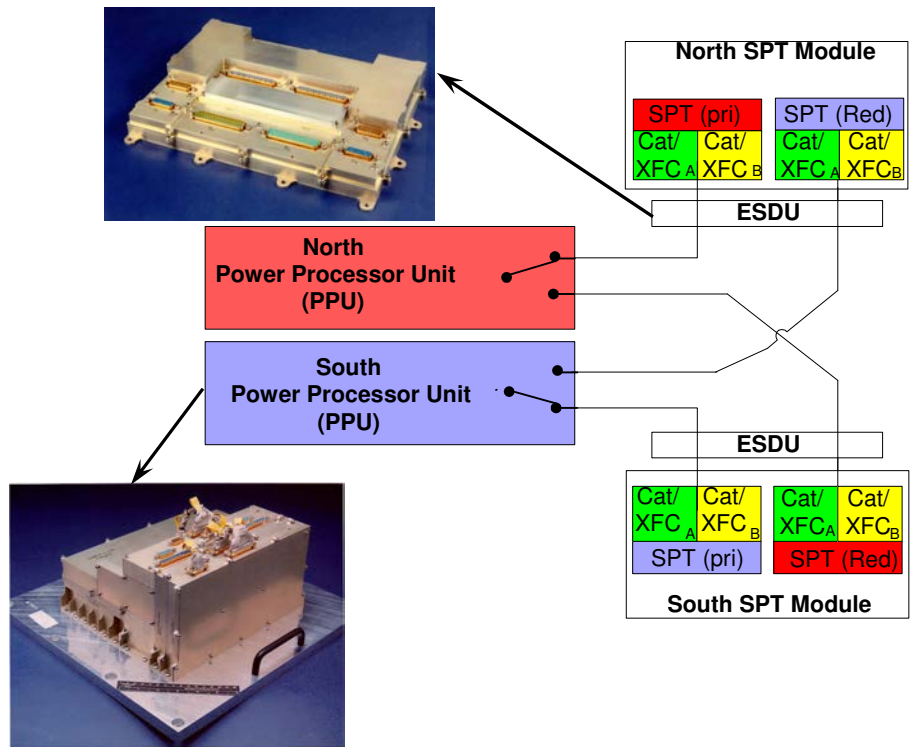
**Figure 2. SPT electrical block diagram.**
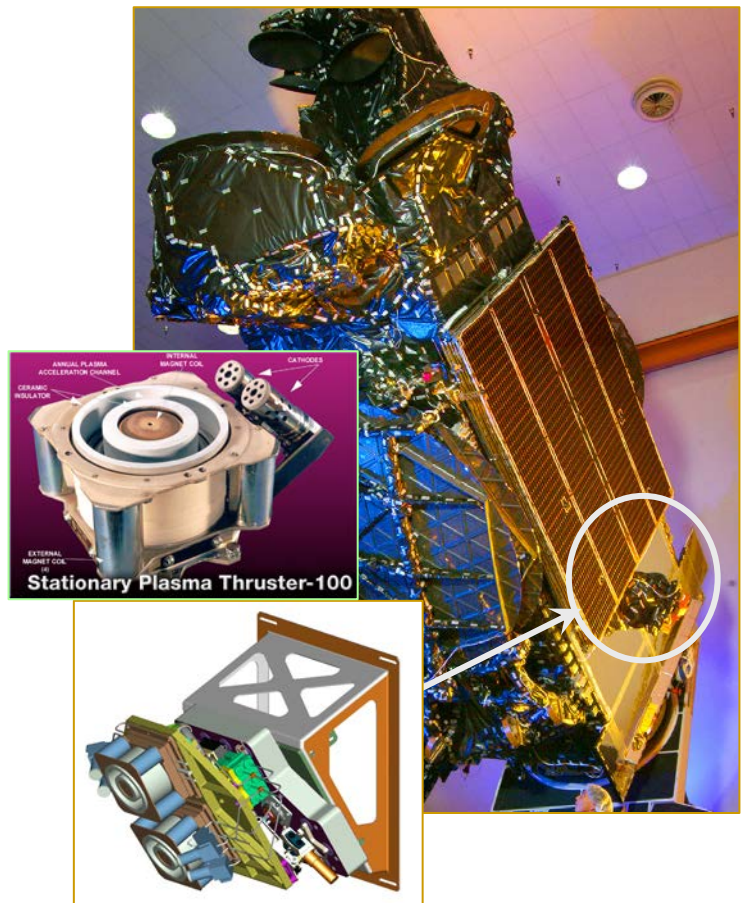


**Figure 3. Stationary Plasma Thruster installation on SPT Gimbal Module with callout to its location on spacecraft communications panel.**
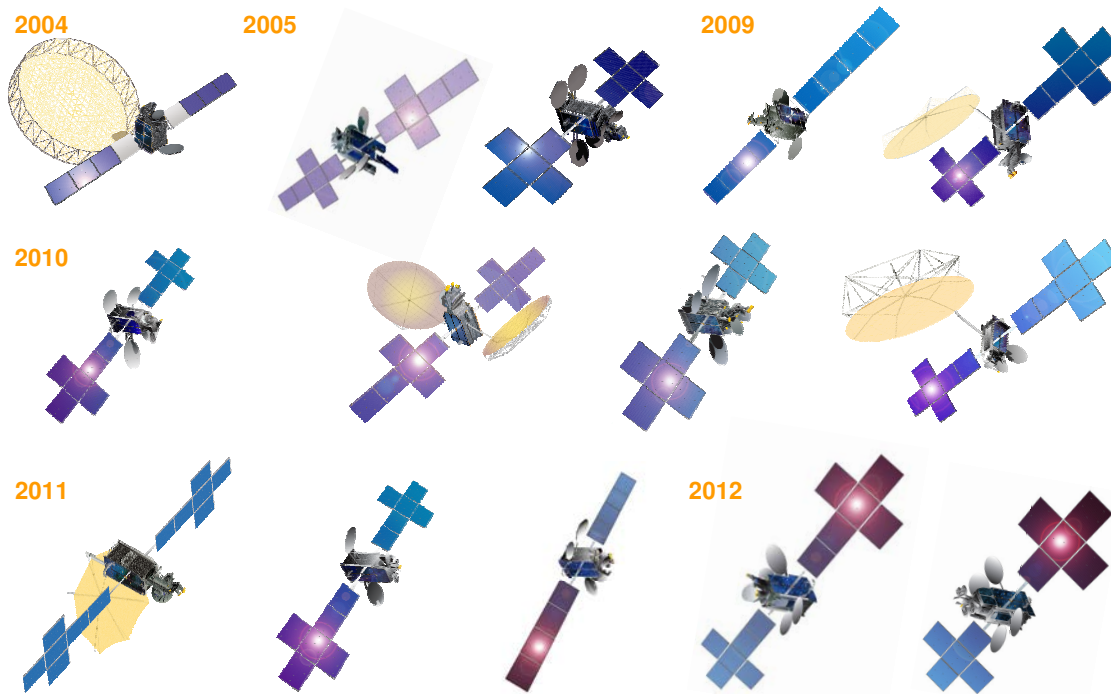
**Figure 4. SS/Ls fleet of SPT-equipped spacecraft in order by launch date.**

An SPT maneuver is executed by following a methodical command sequence that prepares the SPT to be ignited and to sustain the plasma discharge. During a nominal maneuver the sequence starts by opening the PMA latch valve and powering the PPU. At PPU start-up the anode supply is energized first and then the thermothrottle and cathode heaters are powered. At 150 s the XFC selected has all three solenoid valves powered open. After an additional 10 s the cathode igniting electrode pulse train is initiated (350 V amplitude saw-tooth waveform with a period of 80 ms). Once the PPU detects that the thruster has started (discharge current measured is greater than 1.5 A) the PPU turns off the cathode heater, the thermothrottle goes into regulation mode, the igniting electrode is turned off, and the magnet augmentation current is turned on. The SPT typically starts on the first ignition pulse during both ground testing and on orbit.

Performing NSSK maneuvers using SPT-100s (0.083 N thrust) requires a different operational strategy from performing the maneuvers with bipropellant thrusters (22 N thrust). Instead of performing maneuvers every 3-5 weeks, maneuvers are required almost every day. This increase in maneuver frequency and therefore operations workload is offset by several advantages. The largest is the obvious propellant efficiency advantage. Also, the low thrust results in smaller attitude transients during the maneuvers, which increases payload pointing accuracy. The low thrust frees the satellite operator to automate SPT maneuvers without the risks associated with higher thrust maneuvers. This is because unexpected attitude transients that can occur with a high thrust maneuver can cause the spacecraft to quickly lose earth lock. However, unexpected anomalies with a low thrust maneuver can easily be absorbed within the momentum wheels such that they have little or no impact on the payload. Failure detection monitors for an SPT maneuver, if tripped, will terminate the SPT maneuver and the satellite would continue with normal operation. The operator would be notified of the anomaly, and troubleshooting would commence thereafter. Throughout such an event the satellite customers on Earth would not have experienced any interruption of payload service.

With this in mind, SS/L spacecraft incorporate a maneuver table within the on-board software to allow up to 8 days of stored SPT maneuvers. Three data words are required for each maneuver: the start time, the duration of the maneuver, and thruster configuration. After the maneuver table is activated the flight software initiates and executes the SPT maneuvers loaded into the table when their start times are reached. In addition, there are many autonomous safety checks built into the software to terminate the maneuver if anything is out of limits. Significant control exists to tailor the operational profile to the satellite operator's preferences with this maneuver planning strategy. This strategy also enhances operator

convenience in that that no special observation or staffing is required during nominal maneuvers, reducing the operational workload significantly.

Planning and uploading SPT maneuvers is performed by the operator but SS/L provides guidelines to perform this task. Table 1 shows two variations of a daily SPT maneuver strategies that are being implemented by customers operating SS/L spacecraft with SPTs. The specific profile selected is highly dependant on customer ground system software and operational preferences. In both strategies SPTs are operated twice per day separated by approximately 12 hours to perform all NSSK. In the daily strategy, SPT maneuvers are performed every day of the week, as are EWSK maneuvers. Ranging is performed consistently, every day at a low frequency. Orbit determinations are performed once or twice a week, taking the intervening maneuvers into account. Mission planning software then uses these inputs and to calculate a new set of maneuver on-times and durations to be uploaded to the spacecraft maneuver table. In the weekly strategy, SPT maneuvers are only performed 4-5 days a week. Ranging is performed only on the days without any maneuvers, but at a higher frequency. An orbit determination is performed with the ranging information over a time span that also contains no maneuvers. Mission planning software then calculates a EWSK maneuver for the last day of the week and a new set of SPT maneuver on-times and durations to be uploaded to the spacecraft. The weekly strategy does increase the maneuver duration proportionately compared to the daily strategy.

To further reduce operational workload, both the ranging and the maneuver table upload can be automated with ground software. The mission planning software can also incorporate varying degrees of autonomy. With some software, the analyst is only required to initiate the orbit determination and maneuver planning, review the results, and initiate the maneuver table upload (assuming everything is nominal).

**Table 1. SPT On-orbit maneuver strategies.**

| | | Daily Strategy | Weekly Strategy |
|---|---|---|---|
| NS | Thruster | SPT | SPT |
| | Frequency | Twice per day: 1 north, 1 south, every day | Twice per day: 1 north, 1 south, 5 days per week |
| | Duration | 45-50 min per mnvr | 65-70 min per mnvr |
| EW | Thruster | Bi-prop | Bi-prop |
| | Frequency | Shortly after NSSK (as needed) | Every 1-2 weeks, as needed during SPT down time |
| Table Uploading | | Once per week | Once per week |
| Orbit Determination | | Ranging every day, 1-2 ODs per week | Only during non-operational SPT days |

## II. Satellite On-Orbit Performance versus Predictions

The following section discusses a summary of the SPT subsystem hardware qualification and spacecraft interaction testing. Performance parameters measured or analyzed during this ground test campaign such as plume impingement force on the solar array, power degradation through erosion of the solar array, degradation of spacecraft radiator surfaces, and thrust are discussed.

### A. Summary of Ground Test Program

The qualification and life test of the SPT-100 subsystem specifically for Western spacecraft was completed in 1996 by ISTI. Engineering model PPUs were used during the qualification and life testing of the SPT-100 thruster. The power processor development and unit level qualification was performed at SS/L. The propellant management assembly was qualified for ISTI by Moog, Inc. Space Products Division. The details of the SPT subsystem qualification program have been previously reported by Day et. al. [4]. Two SPTs were successfully life tested, the longest exceeding a total impulse of 2.71 million N-sec (or approximately 9000 hours of on-time) and 8872 on/off cycles as described in Garner et. al. [5] and Gnizdor

et. al. [6]. An additional 1000 hour and 700 on/off cycle SPT-100 integrated subsystem qualification test was performed as a final subsystem validation [7]. This test incorporated each of the subsystem components: an SPT-100, two qualification model (QM) xenon flow controller assemblies, the qualification model (QM) PPU, the QM propellant management assembly, and the QM xenon propellant tank were assembled into the life test vacuum chamber at Fakel. The test was performed over a large range of input parameters expected to be seen over the course of a flight mission.

## B. SPT Plume and Spacecraft Compatibility

Consideration of the spacecraft-thruster interactions is necessary when implementing electric propulsion thrusters onto communications satellites. Impingement of high-energy xenon ions (~300 eV) on the spacecraft solar arrays and other surfaces causes torques about the spacecraft center of mass (CM) which must be accounted for and controlled by the spacecraft control system. In addition, surface erosion must also be accounted for in thermal and power budgets.

In order to model these effects SS/L uses an internally developed modeling program to estimate the SPT plume interaction with the spacecraft. SS/L has developed and utilized a model to predict the erosion, redeposition of eroded material, and impingement torques on the spacecraft, allowing proper design of the spacecraft thermal control surfaces, solar array, and control system. The SPT plume model is based on experimental current density and ion energy data taken during ground testing. Sputter yield data, which is necessary to model erosion, was taken from open literature or generated by SS/L under contract with Colorado State University, Fort Collins. Accommodation coefficient values needed to calculate impingement forces were based on values taken from open literature.

A large collection of data has been published over the past decade to document the SPT plume characteristics. The far-field plume contamination and sputtering is found in Randolph [8], the end-of-life plume characterization is found in Pencil [9], and more recent SPT plume characterization data is found in Corey [10] which also gives a detailed discussion of the SS/L impingement torque model.



**Figure 5. Plume model validation using on-orbit plume torque data from Program C. SPT mechanism position as a function of solar array angle (italic values are solar array flight data) [10].**

In addition to ground test data, on-orbit data has been collected with specialized diagnostic sensors on the Express A-2 and Express A-3 geosynchronous communications satellites. This data is summarized in Manzella [11].

## C. Forces and Torques

A model of the SPT plume was developed to analyze the effects of plume impingement on SS/L spacecraft. The development and validation of this model is discussed in detail in Ref. [10]. One aspect of concern is momentum flux from the plume to the spacecraft which creates forces and torques which must be accounted for by the spacecraft control system. Momentum flux is caused by the flow of energetic particles which impinge on spacecraft surfaces. This flux is described by the rate at which the particles arrive (i.e. the plume current density), the energies which they have (i.e. the ion energy distribution function), and the fraction of their momentum which is transferred to the spacecraft upon impact (i.e. the accommodation coefficient).

The orientation of the solar arrays dominates the impingement torque on SS/L spacecraft due to their large area, long moment arms, and location in the SPT plume. The SPT mechanism will move to a positive elevation (smaller cant angle, in direction closer to the solar array) the majority of the time to counter the disturbance roll torque generated by impingement on the solar array. To ensure that the mechanism has adequate range of motion, the predicted impingement torques are used to determine a mechanism mounting

offset. This alignment input is needed to book adequate mechanism range for all phases of the mission including the effect of impingement. If the thruster subsystem is not properly integrated onto the spacecraft (i.e. the thruster is not mounted on the spacecraft so it is correctly aligned with the spacecraft CM) some of the momentum caused by the impinging thruster plume may have to be taken up by the momentum wheels. This momentum would later need to be off-loaded using a chemical propulsion maneuver that would otherwise be unnecessary, which in turn reduces the spacecraft on-orbit mission life.

As discussed previously, the Express on-orbit spacecraft data, summarized in Ref. [11], measured the plume impingement at various solar array angles by reading the reaction torques of the attitude control system while the SPT thrusters were operating. Thus it provides valuable on-orbit data to calibrate the SS/L plume model for forces and torques. Similarly, for the five on-orbit SS/L spacecraft, mechanism motion as a function of solar array angle can be used to calculate the SPT impingement torque which also allows for the plume model to be correlated to flight data.

The predicted mechanism angle is compared to the actual mechanism angle telemetry measured on Program C for different positions of the solar array in Fig. 5. Elevation is in the spacecraft roll direction, and azimuth is in the spacecraft pitch/yaw direction. During SPT operations, the spacecraft control system adjusts the SPT mechanism angle to zero the torque induced by the SPT. The SPT plume impingement torque model shows good correlation with actual on-orbit performance. The two differently sized curves in the figure correspond to the differences of the front versus back side of the solar array material accommodation coefficients. The more specular coverglass side of the array is shown between 90° and 270°, with the back of the array facing the plume at angles from 270° to 90°.

### D. Erosion and Deposition

A model of the SPT plume was developed to analyze the effects of deposition of thruster plume constituents onto spacecraft surfaces, erosion of these surfaces, and the redeposition of this eroded material onto other sensitive surfaces.

The solar array frontside, backside, and edges have to be considered in the erosion analysis because SPT operations encompass nearly all angles of the solar array. The surface of the solar array is made up of many different materials such as solar cell coverglass, room temperature vulcanization (RTV) silicon, Kapton, and graphite. Each of these elements is considered and analyzed within the plume model. The design of the solar array is also modified to ensure the most protection from the SPT plume. Figure 6 shows a sample solar array wing in the plume model workspace. The model integrates the impacts of the plume over the mission, which is typically 15 year for geosynchronous communications satellites. The solar array is also the only moving appendage on the satellite that must be analyzed. The time of the SPT maneuver relative to the solar array angle varies approximately 1 degree per day. This operating scenario is integrated into the model so as to accurately assess the implications of the SPT plume at different solar array angles. There are no SPT firing restrictions relative to solar array angle.

The representative plume model results in Fig. 6 indicate the degree of erosion at different locations on the solar array front-side. Because the solar cell cover glass thickness is orders-of-magnitude greater than the erosion predicted (only a few microns), there is no structural threat. Optically, the properties of the coverglass will not be impacted by the SPT erosion with the exception of the anti-reflective coating applied to the top layer of cover glass. This coating is gradually eliminated by the SPT plume over life. Therefore, at end-of-life, a small percentage of the incident sun light will be reflected and
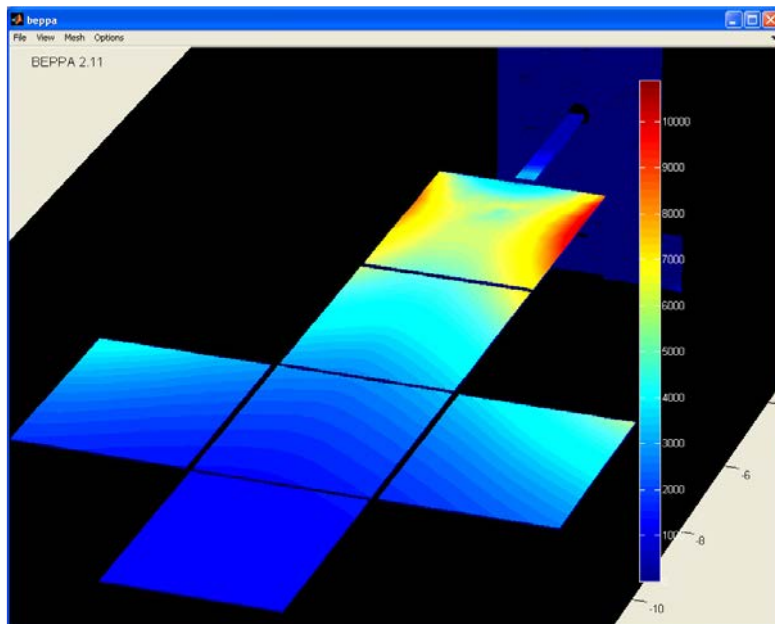


**Figure 6. Representative solar array modeling erosion analysis results used for performance predictions (scale in Å).**

therefore not be available for solar cell power generation. This 2-3% factor is considered and allocated within the system level power budget.

Figure 7 shows the prediction of solar array performance versus the actual measured telemetry for the first years of three missions. The prediction shows both the nominal prediction without the effect of SPT erosion, and the prediction including the effect of SPT erosion. These two lines are within approximately 50 W at this point in life, and eventually will separate to represent the 2-3% difference as discussed above. The actual performance has been tracking the prediction throughout the period shown, and any degradation to date has been undetectable. This validates the plume and solar array modeling and provides confidence that the predicted end-of-life power will be achieved on SS/L SPT spacecraft.
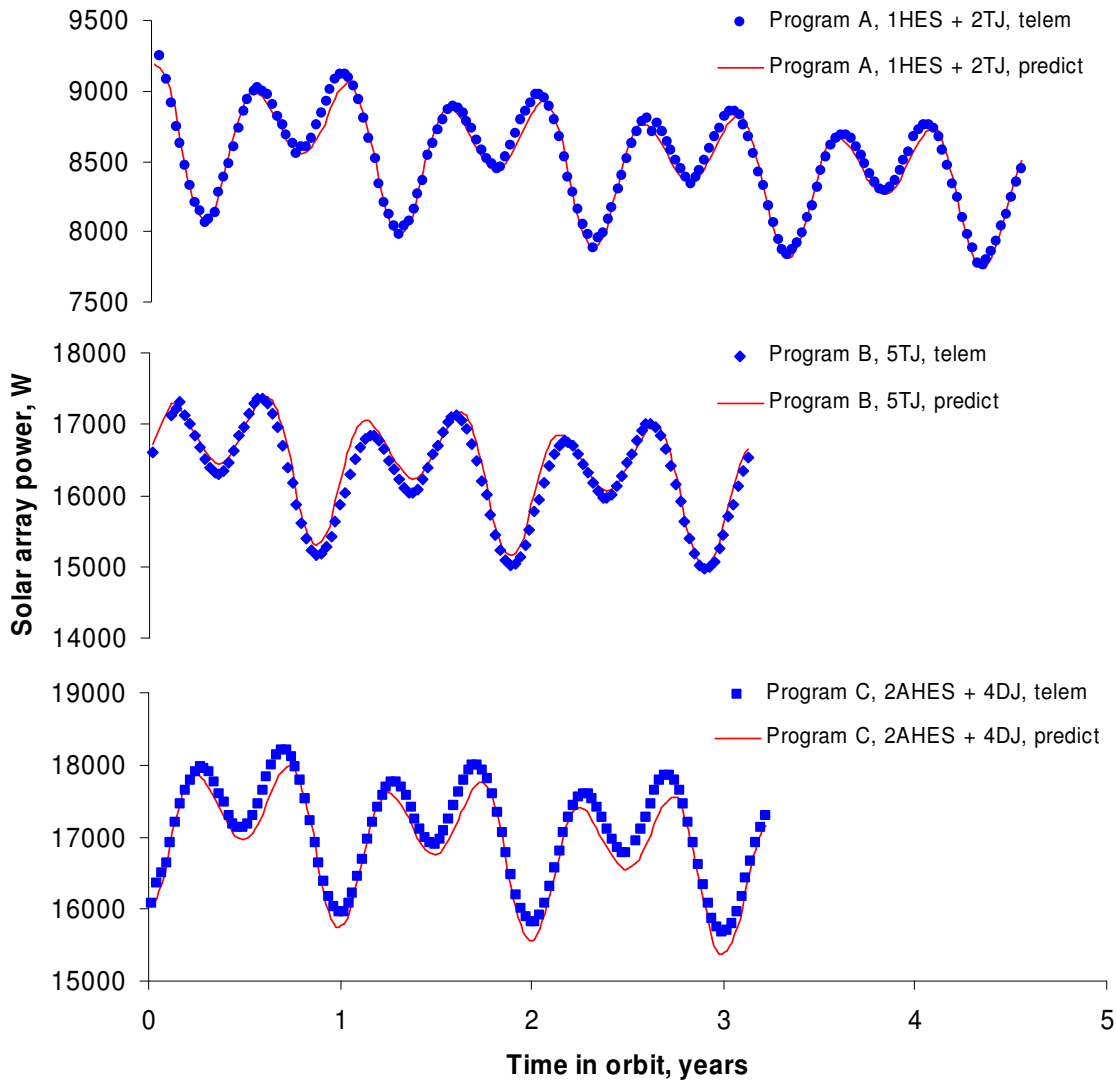


**Figure 7. Solar array performance versus prediction after 5 years in orbit.**

The thermal surfaces of interest external to the spacecraft are the optical solar reflectors (OSR) on the communication panel radiators and thermal blankets. The thermal blankets and OSRs are in the back flow of the SPT plume, i.e. angles greater than 70 degrees from the SPT centerline. There is a small percentage of the thermal radiator that has line of sight to the SPT plume. The impact to the optical properties of the main satellite thermal radiators due to erosion or deposition from the SPT plume is minor or, more quantitatively, the impact to solar absorbtivity is no more than 0.005. On the other hand, there is a large view of the solar array and sometimes reflectors (some of the various satellites that use SPT subsystems also require large deployable reflectors, up to 18 m in diameter as shown in Fig. 4) to the OSRs such that eroded solar array backside material (mostly graphite and black Kapton) and reflector material (mostly molybdenum) is analyzed for redeposition onto thermal surfaces.

Temperature telemetry is being monitored and trended periodically on all SS/L satellites previously launched into orbit. To date, all temperatures are nominal and there is no discernible trend that would indicate anything but normal thermal control system functionality. The thermal predictions using plume model inputs are shown against flight telemetry in Fig. 8. Note that the thermal degradation shown as predicted OSR degradation includes degradation from space environment impacts (UV, and particle radiation) as well as spacecraft material deposition onto the OSRs. The space environment impacts to the OSRs are well known and have been trended over a period of tens of years so the main reason for the difference between predicted and actual shown in Fig. 8 is due to conservatism in the SPT plume model.
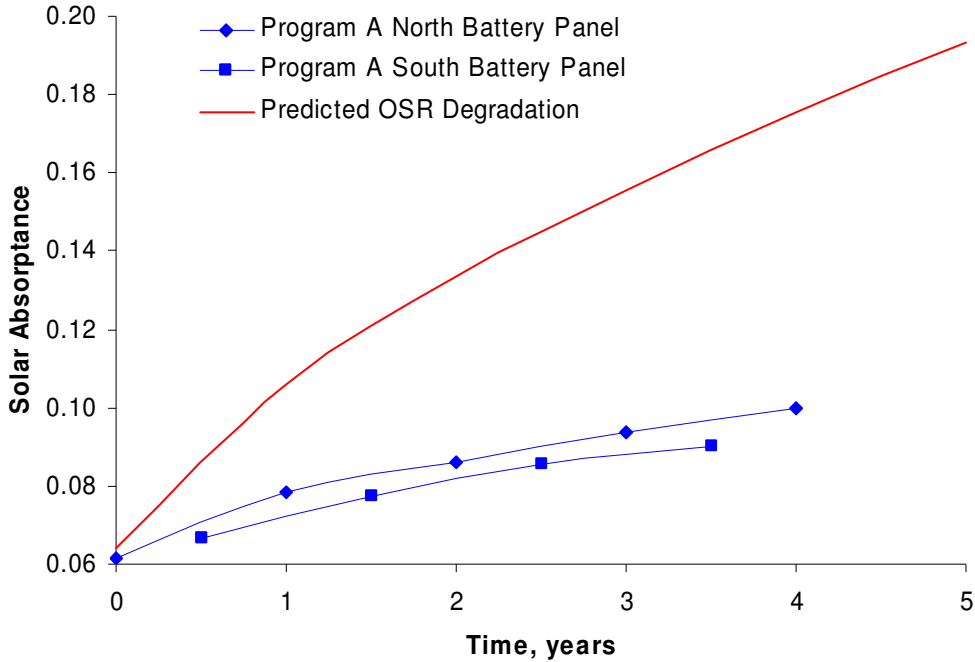


**Figure 8.  Solar array performance versus prediction after 5 years in orbit.**

**E.  Thrust**

The SPT-100 ground test data resulted in an average over life thrust measurement of 83.1 mN, when operated at 4.5 A discharge current. On-orbit thrust is currently not directly measured, but can be estimated from ranging data which is taken during and after each burn. This ranging data is used for orbit determination on a weekly basis as discussed previously. In order to use the ranging data to determine thrust, the expected thrust from the SPT has to be modeled by the orbit determination software. The actual performance (derived from ranging and orbit determination) is compared to the planned maneuver to determine thrust. Measuring thrust in this manner includes errors from the ranging itself, from orbit determination and the assumed thruster thrust model. Due to the multiple sources in measurement error, the total error is difficult to quantify. Errors in orbit determination due to anomalous events (temperature spikes, high solar activity, ground equipment problems) may, at times, cause higher than normal error. This may explain some of the large scatter in the data shown in Fig. 9 where ground tested thrusters (s/n 3 and s/n 5) are compared to on-orbit thrusters (s/n 17 and s/n 18). Over time, some error due to seasonal effects can be identified and may be corrected for. Consistent errors or biases (such as in the assumed thrust model) can also be identified and accounted for. An example of seasonal error can be seen in the periodicity of the data, especially that shown for s/n 17. The SPT thrust performance has been nominal on all SS/L spacecraft, within calculation tolerances.
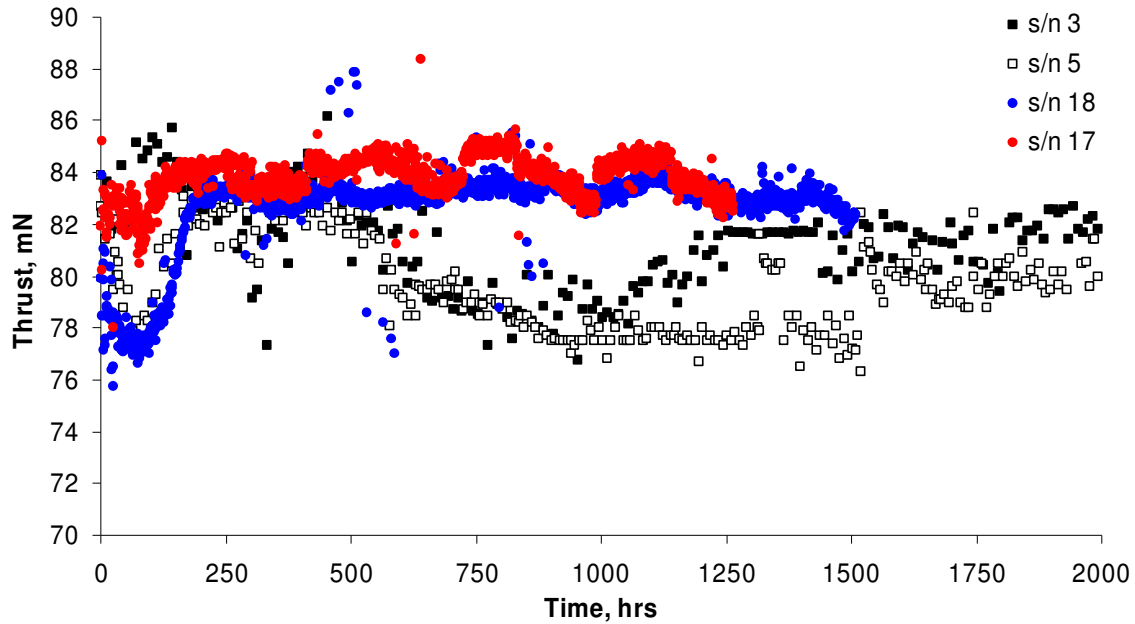
**Figure 9. In orbit thrust compared to ground test unit thrust as a function of on time.**

## F. Electromagnetic Compatibility

The electromagnetic compatibility (EMC) of the SPT subsystem can be separated into a few main subcategories. The most visible and highly studied is the radiated emissions of the SPT and the potential for the emissions to be collected by the communications and command receive subsystems. The second category is conducted EMC from the SPT and PPU back to the power bus. Test programs have been implemented over the period between 1993 and 2003 to fully characterize the EMC of the SPT subsystem at several facilities including Fakel, NASA Glenn Research Center and The Aerospace Corporation.

### 1. Radiated Emissions and Communications Compatibility

Ground testing of the SPT requires testing in a thermal vacuum chamber which introduces many difficulties to achieving clean, unambiguous RF data. A significant improvement was made with facility modifications at The Aerospace Corporation in the late 1990s, which added an RF transparent section to their thermal vacuum tank. This allowed for a more comprehensive evaluation of RF emissions while placing the receive antenna outside the chamber due to easy antennae set-up changes without having to open the vacuum chamber. A very thorough characterization of the radiated spectrum of the SPT is found in Hreha [12]. This evaluation made some important conclusions regarding the RF emissions of SPT-100 thrusters and the implications to end-to-end communications systems analysis. Above 6.5 GHz, there is no detectable radiated emission from the SPT. Therefore, Ku-band and Ka-Band communications systems are not impacted. For C-band payloads, specific communications performance analysis is required to ensure that there is sufficient isolation between the SPT and the uplink feed horns.

The SPT radiated emissions have two main components. One component is a quasi non-coherent background noise emission. The second component consists of pulses that occur sporadically in time, and whose spectral shape closely approximates a chirped continuous wave (CW) radar pulse. From an end-to-end communications systems analysis standpoint, the background noise is considered in the antenna gain-to-thermal noise temperature ratio (G/T) budget as a random noise source possibly degrading the satellites G/T. The sporadic pulses emitted from the SPT are treated as random CW radar pulse interference. The received energy-per-bit to noise ratio (Eb/No) degradation experienced from the pulses can be translated to an effective G/T degradation. In every SS/L application of SPT-100 thrusters the design guidelines applied have resulted in no detectable degradation to communications.

In-orbit testing on the three SS/L spacecraft at S-Band, C-Band, X-Band, Ku-Band, and Ka-Band has not been able to detect any discernable interference. Figure 10 shows on-orbit noise pedestal response test at 5.9 GHz (C-Band) data both with and without SPT operations.

10

**On Orbit Data**

Noise pedestal response **before SPT firing** (5.965 GHz)

5.00 dB/Div

Noise pedestal response **during SPT firing** (5.965 GHz)

5.00 dB/Div
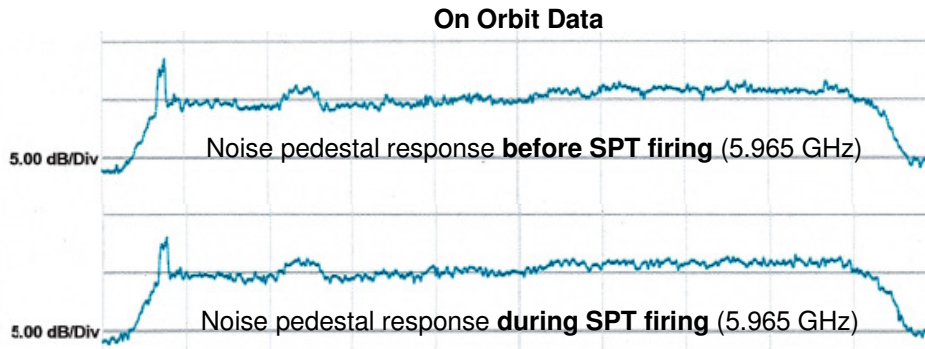
**Figure 10. On-Orbit data for C-band communications showing no discernible indications of SPT interference.**

## 2. Conducted Compatibility

Unlike the radiated emissions aspect to SPT EMC, the conducted nature of the SPT and PPU were directly measured, and therefore power bus compatibility could be tested at subsystem and satellite level test phases. The on-orbit performance is nominal, and transients observed during ignition are well within power bus transient response specifications.

One element of conducted compatibility that was observed on-orbit but was not detected prior to launch was an SPT ignition transient that coupled into the ground plane of the PPU, resulting in saturation and shut-off of a pulse width modulator controlling the PPU auxiliary power supply. This was not observed during development and qualification testing. SPT testing is always performed in a vacuum chamber where the grounding technique is not exactly the same as on the spacecraft. Therefore an unfiltered return line from the thruster to the PPU was vulnerable to ignition noise, but was masked by the vacuum chamber test set-up. Subsequent testing at the Aerospace Corporation to isolate the vacuum chamber structure from between the PPU, SPT, and propellant line was successful at reproducing the shut-off. This modified test set-up better represented the spacecraft grounding. A validation test was successful after a PPU design modification was made, and subsequently demonstrated to work on-orbit. The un-commanded shut-off of the on-orbit PPU has been overcome by accommodating for it within the flight software. This is discussed further in Sec II.I.

## G. Attitude Control System On-Orbit Performance with SPTs

The SPT-100s are mounted to a two-degree of freedom mechanism because of the anticipated movement of the SPT thrust vector relative to the spacecraft. Among the factors that contribute to this are the known drift and uncertainty of the SPT thrust vector as described in Kozubsky [13], the spacecraft center of mass movement as propellant is depleted over life, and the plume impact as discussed above. The satellite attitude control system (ACS) can therefore use the SPT as another actuator while they are in operation. A steering algorithm is used to align the SPT thrust so as to null out the disturbance torque that would result from a mis-pointing of the SPT thrust vector from the center-of-mass. The steering algorithm can also be commanded from the ground station into a momentum management mode of operation. In this mode, the SPT-100 thruster is pointed off from the satellite center of mass in order to remove stored momentum within the ACS. This has the benefit of significantly reducing the quantity of bipropellant thruster wheel unloads, as shown in Fig. 11. Two advantageous consequences of reducing these bipropellant unloads are that bipropellant is saved increasing the satellite's life and the associated attitude transient of a bipropellant thruster actuation is avoided thus improving satellite pointing. The on-orbit attitude and control performance improvement of satellites using the SPT momentum management mode is clearly shown in Fig. 12 in telemetry plots.
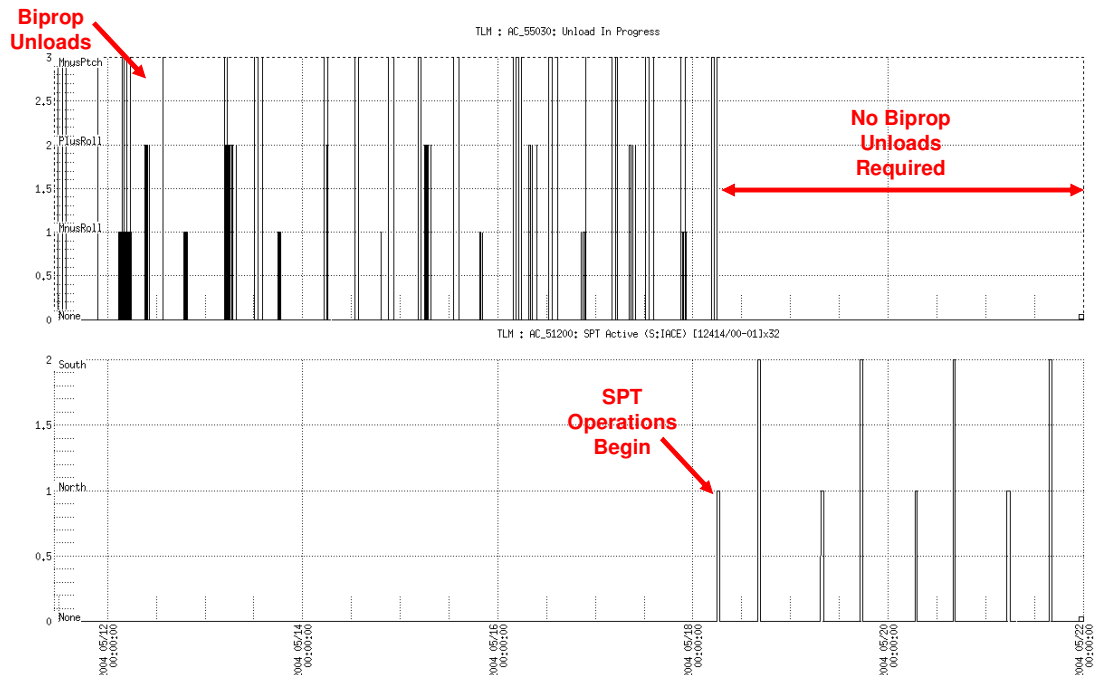
**Figure 11. Attitude control system with SPTs reduces biprop unloads.**
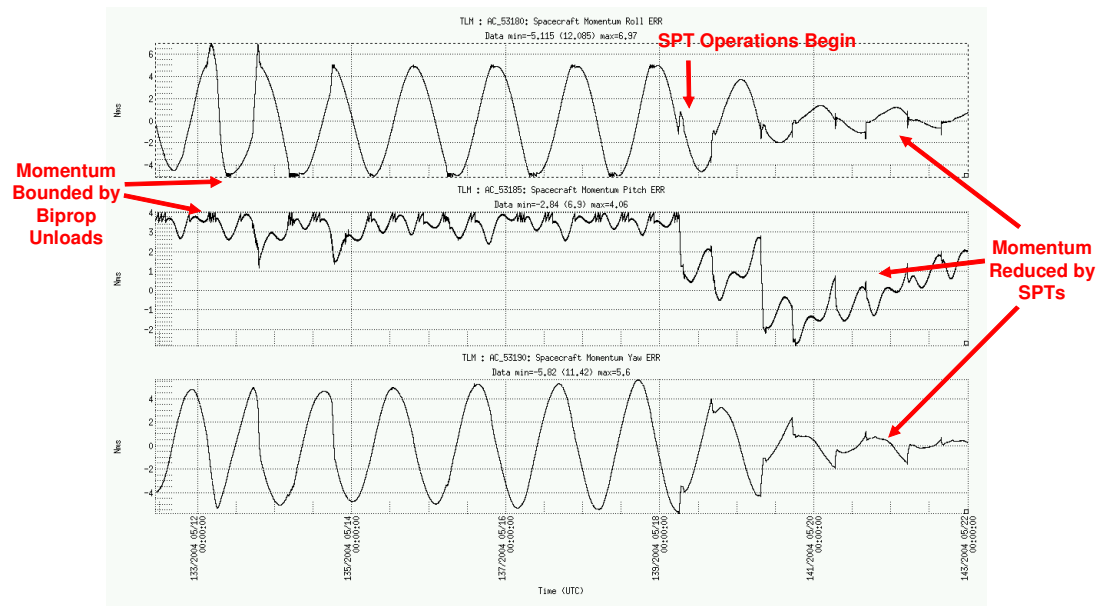


**Figure 12. SPT operations reduce spacecraft momentum errors.**

## H. On-Orbit Data Trending

Trending of quantities not subject to detailed analysis predictions has also been performed. Quantities such as discharge voltage and discharge current which have a nominal value with a tolerance are trended in order to ascertain the general state of health of the subsystem. To accommodate the large amount of data, these items are trended over the course of entire burns and a mean is recorded along with plus or minus one standard deviation ($\pm$ 1$\sigma$). Quantities such as on time and number of cycles have also been trended in order that comparisons can be made to the life test data. This data is summarized in Table 2. Note that discharge

voltage is not trended for programs A, B and C.  This is not an oversight but is because of a change in the way this telemetry was taken in the PPU due to a minor in-flight anomaly discussed in Sec II.I.

Another quantity of interest is the SPT float voltage which is defined as the discharge return referenced to ground.  The SS/L SPT subsystem is designed so that the discharge circuit of the SPT floats with respect to the spacecraft chassis.  The float voltage gives an indication of cathode health.  This quantity is expected to decrease in value over the life of the spacecraft.  Figure 13 shows the cathode float voltage for three programs as a function of time.  Note that there are strong seasonal variations on the cathode float.  This is due to the cathode reacting to exposed voltage on the solar array.  The collection of current by the exposed conductors causes a change in reference which results in the float increasing in value.

**Table 2.  SPT On-time and number of cycles.**

| Total cumalitive on time, hrs | | 9304 |
|---|---|---|
| Total cumalitive cycles | | 8808 |
| Current through | | 15-Aug-09 |

| | | Program A | Program B | Program C | Program D | Program E |
|---|---|---|---|---|---|---|
| Thruster on time | NP | 1674.3 | 1520.6 | 1140.9 | 26.2 | 77.2 |
| | NR | 11.7 | 4.9 | 169.5 | 3.0 | 3.0 |
| | SP | 1464.7 | 1548.3 | 1183.8 | 6.8 | 85.8 |
| | SR | 198.4 | 3.9 | 175.0 | 3.0 | 3.0 |
| | Total | 3349.1 | 3077.7 | 2669.2 | 38.9 | 169.1 |
| Cycles | NP | 1914 | 1376 | 871 | 17 | 124 |
| | NR | 22 | 2 | 122 | 2 | 2 |
| | SP | 1683 | 1370 | 861 | 5 | 112 |
| | SR | 195 | 2 | 124 | 2 | 2 |
| | Total | 3814 | 2750 | 1978 | 26 | 240 |
| Average Discharge Current, A | PPU A | 4.50 | 4.51 | 4.50 | 4.49 | 4.51 |
| | PPU B | 4.51 | 4.54 | 4.50 | 4.52 | 4.45 |
| Standard Deviation, A | PPU A | 0.027 | 0.024 | 0.026 | 0.028 | 0.039 |
| | PPU B | 0.029 | 0.037 | 0.032 | 0.021 | 0.031 |
| Average Discharge Voltage, V | PPU A | | | | 303.3 | 302.3 |
| | PPU B | | | | 302.1 | 301.8 |
| Standard Deviation, V | PPU A | | | | 0.21 | 0.21 |
| | PPU B | | | | 0.18 | 0.20 |
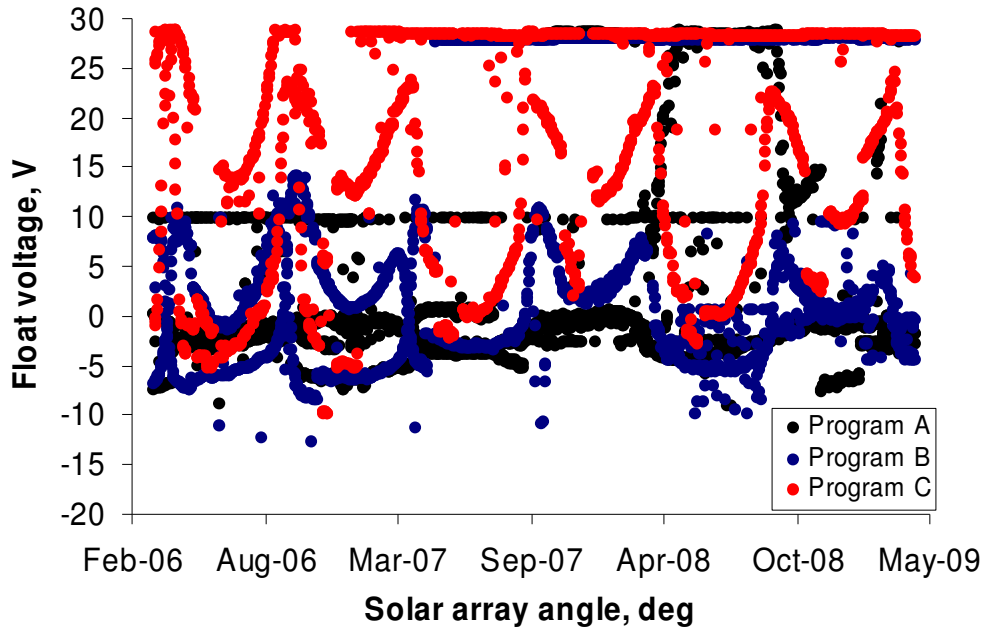
**Figure 13. SPT-100 On-orbit cathode float voltage versus time.**

## I. Anomalies

There has been one major and one minor flight anomaly on SS/L SPT missions. The major anomaly was an uncommanded shutdown of the PPU at the time of SPT start-up and the minor anomaly was a telemetry issue with the float and anode voltage telemetries that caused an overvoltage monitor to trip. In both cases, after the anomaly investigation was compiled and corrective actions implemented, there was no significant impact to the spacecraft mission.

The overvoltage anomaly was shown in telemetry as both the float and anode telemetries going to their full scale high values which are 350 V and 30 V respectively. For the first three spacecraft launched by SS/L, the anode voltage (Dis$^+$) and the cathode float voltage (Dis$^-$) were both referenced to ground (or chassis). SPT discharge voltage was then calculated as Dis$^+$ - Dis$^-$ and this value was checked by a fault detection isolation and recovery (FDIR) monitor. The monitor is set to terminate the SPT burn if the anode voltage or SPT discharge voltage exceeds a predetermined value. After an investigation, it was determined that the root cause of the monitor tripping was that there were exposed conductors on the solar array with voltages up to 100 V. These positive conductors naturally collect current from the SPT plume, and because the spacecraft is electrically floating (and thus must satisfy Kirchhoffs Law), this then causes a change in reference such that when the telemetry circuit measures Dis$^+$ or Dis$^-$ the reference can shift up to 100 V. However, if the reference were to shift by 100 V the telemetry voltage measurements could not reach the actual value of 400 V (300 V + 100 V) for the float telemetry or 100 V (0 V + 100 V) for the anode telemetry but could only reach 350 V and 30 V respectively. Therefore the Dis$^+$ - Dis$^-$ value would be calculated to be 320 V rather than 300 V (e.g. 350 V – 30 V instead of 400 V – 100 V). The corrective action for the anomaly implemented for the spacecraft affected was to disable the FDIR monitor. For the other SPT equipped spacecraft the corrective action was to change the way telemetry was taken so that the PPU measured the anode voltage as Dis$^+$ - Dis$^-$, with only the cathode float voltage (Dis$^-$) being referenced to ground (or chassis). A similar effect on an ion thruster spacecraft is described in [14] and on a Hall thruster spacecraft in [15].

On one of the SPT spacecraft normal SPT start-up and ignition was not always achieved. After a normal warm-up period, at the instant of the ignition, the PPU experienced an un-commanded shut down. The cause was determined to be the pulse width modulator (PWM) in the PPU auxiliary supply latching off due to a noise transient from the SPT into the PPU through the thermothrottle harness. Analysis showed that the latch off did not over-stress the PPU. A ground loop exists in the PPU/SPT that allows induced currents to flow on the thermothrottle wires, which was able to create sufficient noise to latch off the PWM. There is significant variation in the SPT turn on transient such that the PWM latch-off can appear to be a random phenomenon. The PPUs and SPTs have been tested together for thousands of hours and this type of anomaly has never occurred. A possible reason why this anomaly was not observed in ground testing is that vacuum chamber limitations can not reproduce S/C grounding, and discharge within the plasma, e.g.,

the chamber wall is Earth ground while the spacecraft has electrically floating surfaces. Integrated SPT/PPU ground testing was performed with a more representative electrical configuration in order to both reproduce the anomaly and to validate the corrective action. The corrective action was that the PPUs for subsequent missions were equipped with filtering modifications. After this modification, the PPU was qualified, and tested with an SPT. The corrective action for the spacecraft in which this anomaly occurred was to upload a software patch for an auto restart sequence that allows for 2 additional start attempts if the PWM latch-off occurs. An encouraging result that has been proven during these anomalies is that the SPT subsystem has been robust and adaptable even in non-ideal conditions.

## III.  Recent Developments

Recently a full scale qualification and flight of a mechanically actuated large range of motion electric propulsion module was completed by SS/L. The goal of this effort was to develop and qualify an electric propulsion module that could be used over a wide range of spacecraft requirements without sacrificing performance as well as allowing for future growth activities such as electric orbit raising and use of higher power EP thrusters. The SS/L spacecraft that were constructed prior to 2006 utilize SPTs mounted on a gimbaled platform with approximately ±5° of range or motion. This gimbaled platform which is shown in Fig. 3, while a good robust design, but did not allow for future growth, orbit raising (i.e. continuous firing) and integration of larger thrusters such as the SPT-140. The effort was undertaken to develop a new SPT module using an already qualified large range of motion deployment and positioning mechanism (DAPM), to satisfy these and other goals. The Moog manufactured DAPM was qualified by to point antennas on SS/L spacecraft and was first flown in 2005. The development and qualification of this SPT module was intended to capitalize on lessons learned from SS/L's in-orbit experience with its predecessor module. The second-generation SPT module is called the DAPM-actuated SPT module (DSM). The basic features of the design are shown in Fig. 14, and general placement on a typical spacecraft shown (circled) in Fig. 15. To control non-recurring engineering costs (NRE) the final design is limited to 18 options which were required to encompass and meet all possible mission constraints for current and conceived SS/L 1300 series bus spacecraft. There are a total of 9 boom length options and, in addition to boom length variability, mirrored options of these 9 boom lengths are also available giving a total of 18 options. For reference, the DSM shown in Fig. 14 has an option 2 boom and is a counter-clockwise option. The stowage of the module in two axes can be seen in Fig. 15, where the module is shown in its deployed state and the holddown location (refer to Fig. 14) on the spacecraft is just above the pictured technicians head. Also shown in Fig. 14 is the propellant line routing across each axis. Coil number and diameter are both maximized in the space available to provide for the lowest resistive torque to the mechanism possible.

The qualification effort was extensive. The qualification consisted of unit level qualification tests and module level qualification tests. The unit level qualification tests included a holddown delta qualification for higher preload, unit level resistive torque, and cycle life for both the propellant line and harness. The thruster and XFC were also delta qualified for the DSM specific shock environment. Module level qualification tests included environmental and performance.

The first DSM-equipped spacecraft was launched late in
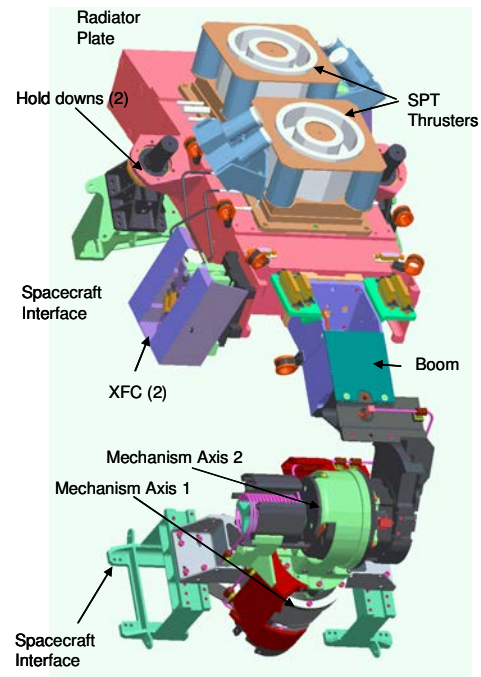


**Figure 14.  DSM overview.**



**Figure 15.  DSM range of motion testing using spacecraft offloader.**

February 2009 on a Land Launch Xenit-3SLB rocket from the Baikanour Cosmodrome in Kazakhstan. After a period of time taken up with chemical orbit raising maneuvers and in-flight systems checks, the DSMs were successfully deployed to the nominal station keeping position in early March. Both DSMs on the spacecraft were successfully deployed from the stowed to nominal stationkeeping position without incident. Following the deployment there was a period of in-orbit testing which included test firings of all four SPTs. There was a long duration burn to verify thermal design and impingement torque predictions over a large range of solar array angles. Everything in the SPT subsystem, including the DSM, performed nominally or better than predictions and the spacecraft has since been handed off to the operator and has entered regular service. Since this time an additional DSM equipped spacecraft has launched and also entered into regular service.

## IV.    Conclusion

Five Space Systems/Loral spacecraft are currently successfully operating SPT-100 thrusters which are performing twice daily SPT maneuvers. Over 9300 SPT on-time hours have been achieved to date on five spacecraft, the first of which has been on-station for over five years. The actual performance for such SPT subsystem parameters as thrust, current, voltage, pressure, and temperature are within tolerance of the specified values. The satellite system performance which could be influenced by SPT operations such as solar array power trend, communications performance, thermal, attitude control, and automated maneuver sequences have been successfully validated and presented herein to the degree possible. Nine more spacecraft currently under construction at SS/L have been designed with the SPT-100 subsystem, and a number of others are in the proposal stage.

The SPT-100 has now successfully flown on 26 spacecraft since 1994, including 9 western spacecraft, totaling 158 SPT-100s, and representing four distinct spacecraft manufactures, Nauchno-Proizvodstvennoe Obiedinenie Prikladnoi Mekhaniki (NPO-PM), Khrunichev State Research and Production Space Center, Astrium and SS/L, each with their own unique power electronics and spacecraft integrated design. The SPT-100 continues to demonstrate its utility and on-orbit reliability.

The SPT subsystem as implemented by SS/L has been robust and adaptable even in non-ideal conditions. Predictive tools have been improved with on-orbit data, and a second generation module has been developed and flown that improves the efficiency of north south station keeping maneuvers, and also provides an adaptable platform for future electric orbit raising operations.

## V.    Acknowledgements

## VI.    References

[1]  Pidgeon, D., "System benefits and Satellite Accommodations of the Stationary Plasma Thruster", AIAA 94-1008, 15th International Communications Satellite Systems Conference, San Diego, California, 1994.
[2]  Goebels, D. M., and Katz, I., *Fundamentals of Electric Propulsion: Ion and Hall Thrusters*, John Wiley and Sons, New Jersey, 2008.
[3]  Morozov, A. I. and Savelyev, V. V., *Fundamentals of Stationary Plasma Thruster Theory*, Reviews of Plasma Physics 21, Kluwer Academic/Plenum Publishers, New York, 2000.
[4]  Day, M., Maslennikov, N., Randolph, T., Rogers, W., "SPT-100 Subsystem Qualification Status", AIAA-96-2713, 32nd Joint Propulsion Conference, Lake Buena Vista, Florida, 1996.
[5]  Garner, C. E., Brophy, J. R., Polk, J. E. , Pless, L. C., and Starling, D. A., "A 5730-Hr Cyclic Endurance Test of the SPT-100," IEPC-95-179, 1995.
[6]  Gnizdor, R., Kozubsky, K., Koryakin, A., Maslennikov, N., Pridannikov, S., and Day, M., "SPT100 Life Test with Single Cathode up to Total Impulse Two Million Nsec," AIAA-98-3790, 1998.
[7]  Randolph, T., Fischer, G., Pidgeon, D., Rogers, W., Staley, M., Day, M., et al, "Integrated Test of an SPT-100 Subsystem," AIAA-97-2915, 33rd Joint Propulsion conference, Seattle, WA, July, 1997.
[8]  Randolph, T., Pencil, E. J., and Manzella D. H., "Far-Field Plume Contamination and Sputtering of the Stationary Plasma Thruster," AIAA-94-2855, 1994.
[9]  Pencil, E. J., Randolph, T. M., and Manzella, D. H., "End-of-Life Stationary Plasma Thruster Far-Field Plume Characterization," AIAA 96-2709, 1996.

[10] Corey, R. L., Price, X., Malone, S. M, Randolph, T., M and Snyder, J., S., "Hall Thruster Plume Model for Spacecraft Impingement Torque: Development and Validation" *Journal of Spacecraft and Rockets*, Vol. 45, No. 4, 2008, pp. 766-775.

[11] Manzella, D., Jankovsky, R., Elliot, F., Mikellides, I. Jongeward, G. and Allen, D., "Hall Thruster Plume Measurements On-board the Russian Express Satellites," IEPC paper, 2001-044, October 2001.

[12] Hreha, W., Singh, R., Liang, S., Burr, D., Day, M., "SPT Interference Assessment in Communications Satellites", AIAA 2004-3216, 2004.

[13] Kozubsky, K., Zhurin V. V., and Higham, J. S. "Disturbance Torques Generated by the Stationary Plasma Thruster," AIAA-93-2394, 1993.

[14] Brinza, D. E., Henry, M. D., Mactutis, A. T., McCarty, J. D., vanZandt, T. R., Wang, J. J., Tsurutani, B. T., Katz, I., Davis, V. A., Musmann, G., Richter, I., Othmer, C., Glassmeier, K., and Moses, S., "Ion Propulsion Subsystem Environmental Effects on Deep Space One: Initial Results from the IPS Diagnostic Subsystem DS1 Technology Validation Report," Deep Space 1 Technology Validatation Symposium, Pasadena, CA, 2004.

[15] Scharlemann, C., Tajmar, M., Gonzalez, J., Estublier, D., Noci, G., and Carpacci, M., "Influence of the Solar Arrays on the Floating Potential of SMART-1: Numerical Simulations," AIAA-2005-3859, 41st Joint Propulsion Conference, Az, 2002.